Melting and Octupole Deformation of Na_{40}

A. Rytkönen, H. Häkkinen,* and M. Manninen

Department of Physics, University of Jyväskylä, P.O. Box 35, FIN-40351 Jyväskylä, Finland

(Received 20 January 1998)

The dynamics and electronic structure of the magic Na_{40} cluster are studied as a function of temperature using an *ab initio* molecular dynamics method. Na_{40} is found to undergo a structural transition which can be identified as melting by traditional indicators. Melting transition was observed in the region 300–350 K with a latent heat of melting of 11 meV/atom, which is 42% of the bulk value. Octupole deformation is the dominating type of multipole deformations in the temperature range studied (150–550 K). The stability of the deformation type is indicated by the persistently large HOMO-LUMO gap, both in the solid and liquid phases. [S0031-9007(98)05983-3]

PACS numbers: 36.40.Cg, 36.40.Ei, 36.40.Mr

Progress in experimental methods has made it possible to study the solid-liquid transition of free metal clusters [1,2]. In a recent study [2], the melting temperature and latent heat of melting of Na_{139}^{+} have been determined. It can be expected that phase transitions of even smaller alkali metal clusters can be studied in the near future.

Theoretically, melting of finite systems has been studied intensively during the past, and computer simulations have given new information about structural transitions in various cluster types [3]. However, there are only a few theoretical studies on melting and isomerization of sodium clusters even though sodium is an important reference system because it is well described with the jellium model [4,5]. Some studies have used a tight-binding formulation of the Hamiltonian combined with Monte Carlo [6] or molecular dynamics with a phenomenological many-body potential [7]. Simple model studies have been performed for sodium clusters with up to 800 atoms [8]. Röthlisberger and Andreoni [9] have performed Car-Parrinello *ab initio* calculations of finite-temperature properties of sodium clusters with 2–20 atoms. To date, however, no detailed electronic structure calculation of dynamical properties of metal clusters has been reported for sizes large enough that melting can be convincingly identified and separated from isomerization [2].

In this Letter we have studied the finite-temperature dynamics of Na_{40} including both electronic and structural properties with the *ab initio* BO-LSD-MD (Born-Oppenheimer, local-spin-density, molecular dynamics) method devised by Barnett and Landman, fully documented in Ref. [10]. As the kinetic temperature of the cluster is increased, the cluster undergoes a melting transition, distinctly different from the structural isomerization observed in smaller alkali metal clusters [11], in a temperature region that agrees reasonably well with experimentally determined melting temperature of Na_{139}^{+} [2]. The octupole deformation is found to be the dominating type of multipole deformation at low temperatures and, as the cluster melts, it is further enhanced. This deformation results in the magic nature of Na_{40}.

In the BO-LSD-MD method one solves the Kohn-Sham (KS) one-electron equations for the single-electron states of the valence electrons of the system corresponding to a given nuclear configuration of the ions. From the converged solution the Hellman-Feynman forces on the ions can be calculated which, together with the classical Coulomb repulsion between the positive ion cores, determine the total forces on the ions, according to which classical molecular dynamics for the ions is performed. The fully converged solution for the electronic structure is obtained for each successive ionic configuration, which ensures that the positions of the ions are advanced in such a manner that the whole system follows dynamics on the Born-Oppenheimer energy surface. The current implementation uses plane waves combined with fast Fourier transform techniques as the basis for the one-electron wave functions and norm-conserving, nonlocal, separable [12] pseudopotentials by Troullier and Martins [13,14] to describe the valence electron-ion interaction, and the LSD parametrization by Vosko, Wilk, and Nusair [15].

The shape of the cluster was analyzed in terms of a multipole expansion [16]. The strength of each multipole component was determined by using dimensionless shape parameters S_l defined as

$$S_l = \sum_{m=-l}^{l} |a_{lm}|^2 = \sum_{m=-l}^{l} \frac{4\pi(2l+1)}{9 r_s^{2l} N^{2l/3+2}} |Q_{lm}|^2, \qquad (1)$$

where the multipole moments Q_{lm} are defined as

$$Q_{lm} = \sqrt{\frac{4\pi}{2l+1}} \int d^3r\, r^l Y_{lm}(\theta,\phi) n(\mathbf{r}), \qquad (2)$$

where Y_{lm} is a spherical harmonic, $n(\mathbf{r})$ is the valence electron density, and r_s is the density parameter of the electron gas. The details of this formulation are presented in [16]. When defined in this way, all possible values of m are included in each S_l, making it rotationally invariant. The shape parameters are calculated during a molecular dynamics run for $l = 2$, 3, and 4, corresponding to quadrupole,

 0031-9007/98/80(18)/3940(4)$15.00

octupole, and hexadecupole deformations of the cluster, respectively.

In the present study, the kinetic temperature of the cluster was slowly raised by scaling the velocities of the ions. As a starting configuration, we used 40 atoms having icosahedral structure; a 55 atom complete icosahedron minus all of the 12 corner atoms and one (111) facet. This is the most spherical structure one can construct for 40 atoms having icosahedral structure. This structure soon transformed into an energetically more favorable structure which is described later in this paper. The cluster was heated linearly from 150 to 400 K at a heating rate of 5 K/ps and, for comparison, from 250 to 400 K at a heating rate of 2.5 K/ps. One should note that these heating rates are still so high that a true thermal equilibrium is not reached during the simulations. Here we concentrate on the results of the 5 K/ps heating run. In addition, a constant energy simulation of the cluster at approximately 550 K was performed to study the properties of the cluster at a higher temperature.

Figure 1(a) shows the mean square displacement of the atoms, $R^2(t) = \sum_{i=1}^{N} |\mathbf{r}_i(t) - \mathbf{r}_i(0)|^2/N$, as a function of time (temperature), calculated with respect to their positions at $T = 190$ K. The mean square displacement starts to increase approximately at 300 K. The approximate diffusion coefficient in the temperature region 300–400 K is 0.2×10^{-4} cm^2/s, which is comparable to a typical bulk liquid diffusion coefficient of 10^{-5} to 10^{-4} cm^2/s. For comparison, we obtained for Na_{40} a value of 0.5×10^{-4} cm^2/s at 550 K, and Röthlisberger and Andreoni [9] deduced a value of 0.5×10^{-4} cm^2/s for Na_{20} at 640 K. Figure 1(b) shows the time evolution of the potential energy. The curve is constructed by averaging each data point, taken every time step (5 fs), over a time period of 0.5 ps to display the principal features. When compared with Fig. 1(a), one can see that the potential energy increases by approximately 11 meV per atom around the temperature where the mean square displacement starts to increase. Even though the curve shows large fluctuations after the transition, reflecting the broadening of the transition in this finite system (and the fact that the thermal average is not reached), it is evident that it has reached a level and slope different from those in the low-temperature solid phase.

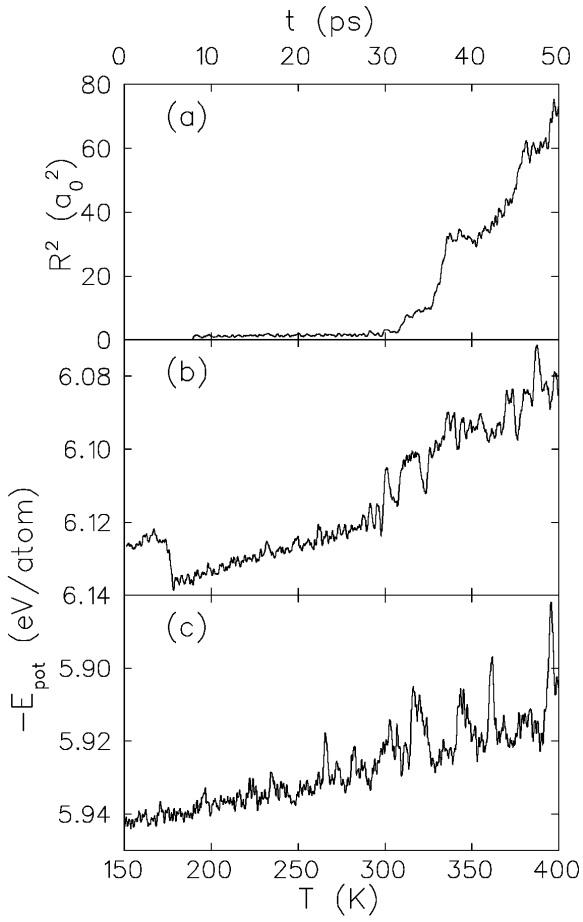

FIG. 1. (a) Mean square displacement of Na_{40} cluster and (b) potential energy of Na_{40}; (c) Na_8 cluster as a function of time (temperature) in the heating run of 5 K/ps.

For comparison, Fig. 1(c) shows the potential energy curve for Na_8 [17], heated at the same rate and the data averaged in the same way as for Na_{40}. Unlike in the case of Na_{40}, the curve shows no transition region taking the potential energy of the cluster to a higher level. Na_8 is found to visit isomers lying higher in energy, but is not observed to remain there. The difference between the curves 1(b) and 1(c) shows that, below the bulk melting temperature of 371 K, Na_{40} shows a rounded transition that can be identified as melting, while Na_8 exhibits only isomerization.

In a bulk system, the melting transition is conventionally detected with a discontinuity in the caloric curve at a certain temperature. Another criterion for the melting transition is the difference between the behavior of the mean square displacement in solid and liquid phases: In the solid phase, the mean square displacement fluctuates around a constant value, but in liquid phase it has a constant positive slope. In a finite system, the transition is rounded [18] and, instead of exhibiting a single melting temperature, the system has a finite-temperature region at which it can exist in either solid or liquid phase, the probability of the other vanishing exponentially as the region boundary is approached. As the cluster is heated linearly at a finite rate, the melting transition may happen anywhere in the melting region in a single simulation. Based on our simulations, we can, however, present a reasonable estimate for the range of the melting region.

The heating simulation of Na_{40} was repeated using a heating rate of 2.5 K/ps. With this heating rate, the cluster was observed to melt at about 350 K, exhibiting the same diffusion coefficient and latent heat of melting as in the simulation done with 5 K/ps. On the basis of these calculations, we conclude that the width of the melting region for Na_{40} is at least 50 K.

Below the transition region, the potential energy curve is linear and yields a constant heat capacity of 0.25 meV/K per atom for both heating rates. Theoretically, Poteau *et al.* [6] obtained for the heat capacity for Na_8 0.23 meV/K and for Na_{20} 0.25 meV/K, while the heat capacity of Na_{139}^+ was experimentally determined to be 0.23 meV/K [2]. These values are comparable with the Dulong-Petit value 0.26 meV/K. Although the statistics of our simulations is not good enough to determine an accurate caloric curve, both heating simulations resulted in the same latent heat of melting of 11 meV per atom for Na_{40}. Schmidt *et al.* [2] obtained 14 meV per atom for Na_{139}^+. These are much smaller than the bulk value 27 meV per atom [19] due to the large surface-to-volume ratio.

Figure 2 shows the density of Kohn-Sham single-electron states as a function of energy at different temperature regions. The density of states for the spherical starting configuration is displayed in Fig. 2(a). The electronic structure is consistent with the spherical jellium picture [4,5], exhibiting large energy gaps at 8, 20, and 40, and small but clear gaps at 18 and 34. Figure 2(b) shows the density of states before and after melting. As the cluster melts, the shells are broadened but the principal features remain the same. The HOMO-LUMO (highest occupied molecular orbital–lowest unoccupied molecular orbital) gap remains broad, approximately 0.4 eV. Figure 2(c) shows the density of states at 550 K, where the shell structure is still recognizable.

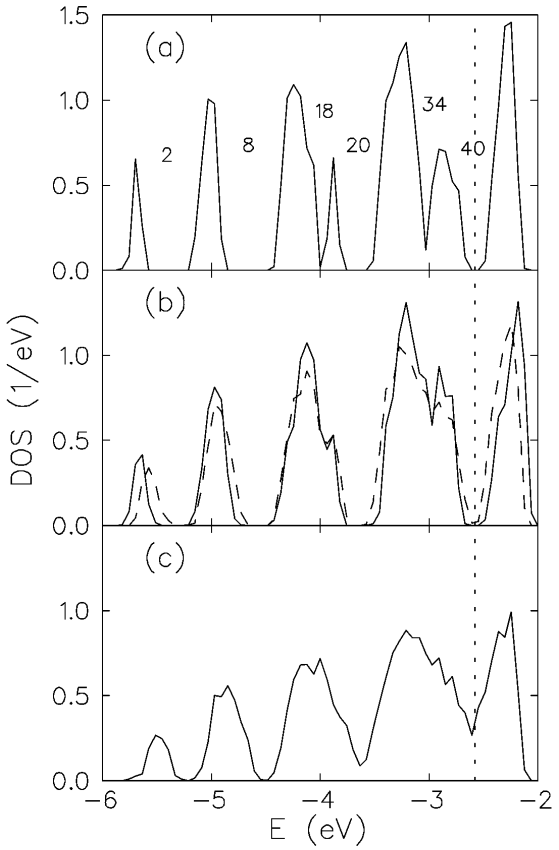

FIG. 2. Density of KS states for (a) initial "spherical" cluster, (b) octupole-deformed solid (solid curve) and melted (dashed curve) cluster, and (c) liquid cluster at 550 K. The vertical dotted line denotes the HOMO-LUMO gap. Also, the shell-closing electron numbers are shown in (a).

After 5 ps of heating, at about 175 K, the cluster was observed to transform into an energetically more favorable structure [Figs. 1(b) and 3]. It contains three decahedra on top of each other, rotated $\pi/5$ radians with respect to each other. The rest of the atoms are distributed around the decahedra at sites determined by the fivefold symmetry. This structure is 13 meV/atom lower in energy than the icosahedral starting configuration and is observed to persist at all temperatures below the melting transition. Its relative stability with respect to the icosahedral structure is also indicated by the change in the KS energy levels. The jellium-type gaps at 18 and 34 are observed to narrow while the HOMO-LUMO gap is broadened [compare Fig. 2(a) and the solid curve in Fig. 2(b)]. It is undoubtedly a stable structure for Na_{40} at low temperatures.

The evolution of the shape parameters S_l, $l = 2$–4, is shown in Fig. 4. At the beginning of the simulation, all S_l values are relatively small, reflecting the spherical shape. As the cluster finds the low-energy structure of Fig. 3, the octupole deformation is enhanced with respect to quadrupole and hexadecupole deformations. At the melting transition region, the octupole deformation is further enhanced and, in fact, its average value is doubled. This is in agreement with the calculations of Hamamoto *et al.* [20], done with a modified oscillator model, indicating that the octupole deformation is significant for Na_{40}, and should dominate over the spherical shape. At 550 K, the octupole deformation still persists as the dominating deformation type (not shown).

It has been shown before [21] that small liquid alkali clusters can have strong deformation stabilized by the shell structure. It is interesting to note that Na_{40} *spontaneously octupole deforms* at relatively low temperature and the energy difference between a spherical and octupole-deformed structure is so clear [see the beginning of the potential energy curve in Fig. 1(b)]. The octupole deformation diminishes the energy gap at 34 electrons and increases the HOMO-LUMO gap. This is the main reason for 40 being

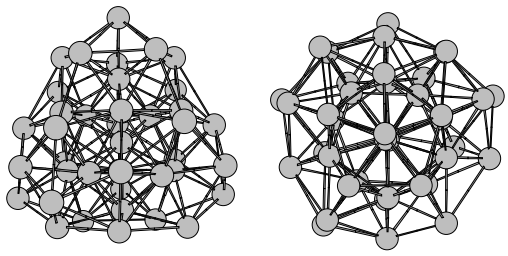

FIG. 3. Structure of the octupole-deformed low-temperature cluster, shown from two mutually orthogonal directions. The structure is obtained by averaging the atomic positions over 1.5 ps at approximately 190 K.

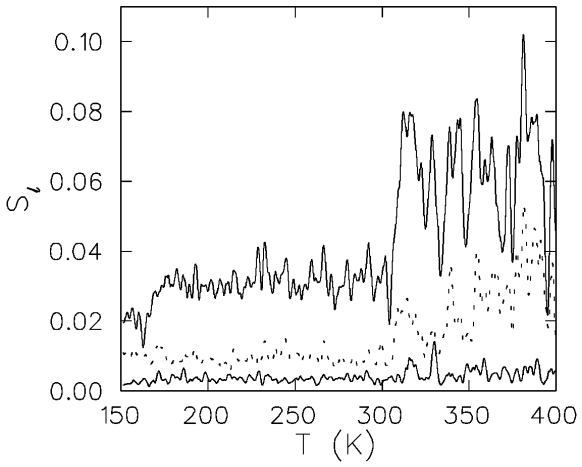

FIG. 4. Shape parameter vs temperature for quadrupole ($l = 2$, lower solid curve), octupole ($l = 3$, higher solid curve) and hexadecupole ($l = 4$, dotted curve) deformation.

a strong magic number instead of 34, and confirms earlier anticipations [22].

Schmidt *et al.* [2] obtained for Na_{139}^{+} a melting temperature of 267 K, which is below the melting temperatures 300 and 350 K obtained here for the two simulations of Na_{40}. This may be caused by the electronic stability of Na_{40} and also the stabilizing effect of the octupole deformation. It also suggests that the melting temperature of sodium cluster is not a monotonous function of atomic number, but instead the stabilizing effect of the electronic structure may raise the melting temperature considerably for smaller magic clusters.

In summary, we have studied melting, multipole deformations and electronic structure of sodium cluster with 40 atoms using the BO-LSD-MD method. Na_{40} is observed to exhibit a rounded melting transition at about 300–350 K with a latent heat of melting of 11 meV/atom, contrary to the mere isomerization observed in smaller alkali clusters. These results agree well with a recent experiment on Na_{139}^{+} [2]. At the wide temperature range of our study, Na_{40} is found to be dominantly octupole deformed. The HOMO-LUMO gap remains broad at temperatures below 400 K, displaying the electronic stability of the cluster.

This work is supported by the Academy of Finland.

*Present address: School of Physics, Georgia Institute of Technology, Atlanta, GA 30332.

[1] T. P. Martin, U. Näher, H. Schaber, and U. Zimmermann, J. Chem. Phys. **100**, 2322 (1994).
[2] M. Schmidt, R. Kusche, W. Kronmüller, B. von Issendorff, and H. Haberland, Phys. Rev. Lett. **79**, 99 (1997).
[3] J. D. Honeycutt and H. C. Andersen, J. Phys. Chem. **91**, 4950 (1987); J. P. Rose and R. S. Berry, J. Chem. Phys. **98**, 3246 (1993); S. Valkealahti and M. Manninen, Comput. Mater. Sci. **1**, 123 (1993); O. B. Christensen and K. W. Jacobsen, J. Phys. Condens. Matter **5**, 5591 (1993); Q. Wang, M. P. Iñiguez, and J. A. Alonso, Z. Phys. D **31**, 299 (1994); C. L. Cleveland, U. Landman, and W. D. Luedtke, J. Phys. Chem. **98**, 6272 (1994); S. Valkealahti and M. Manninen, J. Phys. Condens. Matter **9**, 4041 (1997); A. Rytkönen, S. Valkealahti, and M. Manninen, J. Chem. Phys. **108**, 5826 (1998).
[4] W. A. de Heer, Rev. Mod. Phys. **65**, 611 (1993).
[5] M. Brack, Rev. Mod. Phys. **65**, 677 (1993).
[6] R. Poteau, F. Spiegelmann, and P. Labastie, Z. Phys. D **30**, 57 (1994).
[7] N. Ju and A. Bulgac, Phys. Rev. B **48**, 2721 (1993).
[8] A. Maiti and L. M. Falicov, Phys. Rev. A **45**, 6918 (1992).
[9] U. Röthlisberger and W. Andreoni, J. Chem. Phys. **94**, 8129 (1991).
[10] R. N. Barnett and U. Landman, Phys. Rev. B **48**, 2081 (1993).
[11] V. Bonačić-Koutecký, J. Jellinek, M. Wiechert, and P. Fantucci, J. Chem. Phys. **107**, 6321 (1997).
[12] L. Kleinman and D. M. Bylander, Phys. Rev. Lett. **48**, 1425 (1982).
[13] N. Troullier and J. L. Martins, Phys. Rev. B **43**, 1993 (1991).
[14] A kinetic energy cutoff $E_c^{\mathrm{PW}} = 5.6$ Ry is used for the plane-wave basis set.
[15] S. H. Vosko, L. Wilk, and M. Nusair, Can. J. Phys. **58**, 1200 (1980); S. H. Vosko and L. Wilk, J. Phys. C **15**, 2139 (1982).
[16] M. Koskinen, P. O. Lipas, and M. Manninen, Z. Phys. D **35**, 285 (1995).
[17] H. Häkkinen (unpublished).
[18] H. Reiss, P. Mirabel, and R. L. Whetten, J. Phys. Chem. **92**, 7241 (1988); H.-P. Cheng, X. Li, R. L. Whetten, and R. S. Berry, Phys. Rev. A **46**, 791 (1992); D. H. E. Gross, M. E. Madjet, and O. Schapiro, Z. Phys. D **39**, 75 (1997).
[19] *CRC Handbook of Chemistry and Physics*, edited by R. C. Weast (CRC Press, Boca Raton, 1986).
[20] I. Hamamoto, B. Mottelson, H. Xie, and X. Z. Zhang, Z. Phys. D **21**, 163 (1991).
[21] H. Häkkinen and M. Manninen, Phys. Rev. B **52**, 1540 (1995).
[22] S. M. Reimann, M. Koskinen, H. Häkkinen, P. E. Lindeløf, and M. Manninen, Phys. Rev. B **56**, 12 147 (1997).